Mixed-sensitivity approach to H∞ control of power system oscillations employing multiple FACTS devices

Mixed-Sensitivity Approach to H_∞ Control of Power System Oscillations Employing Multiple FACTS Devices

Balarko Chaudhuri, Bikash C. Pal, Argyrios C. Zolotas, Imad M. Jaimoukha, and Tim C. Green

***Abstract*—This paper demonstrates the enhancement of inter-area mode damping by multiple flexible ac transmission systems (FACTS) devices. Power system damping control design is formulated as an output disturbance rejection problem. A decentralized H_∞ damping control design based on the mixed-sensitivity formulation in the linear matrix inequality (LMI) framework is carried out. A systematic procedure for selecting the weights for shaping the open loop plant for control design is suggested. A 16-machine, five-area study system reinforced with a controllable series capacitor (CSC), a static var compensator (SVC), and a controllable phase shifter (CPS) at different locations is considered. The controllers designed for these devices are found to effectively damp out inter-area oscillations. The damping performance of the controllers is examined in the frequency and time domains for various operating scenarios. The controllers are found to be robust in the face of varying power-flow patterns, nature of loads, tie-line strengths, and system nonlinearities, including device saturations.**

***Index Terms*—FACTS, H-infinity control, inter-area oscillations, LMI, model reduction, robustness.**

I. Introduction

INTER-AREA oscillations (0.2–1.0 Hz) are inherent in large interconnected power systems [1]. The present business environment of the electricity supply industry is encouraging more long distance power trading which is increasingly putting stress on the existing transmission systems. As a result, damping of the inter-area modes tends to degrade with increasing maximum power transfer across tie-lines, exciting the low frequency oscillations. The incidents of system outage resulting from these oscillations are of growing concern [1]. Over the last three decades, attention has been focussed on designing controls to damp out these oscillations. The traditional approach to damping inter-area oscillations is through installation of power system stabilizers (PSS's) [2] that provide supplementary control action through excitation control of the generators. In recent times, the use of FACTS devices has become a common practice in order to make full utilization of the existing transmission capacities instead of adding new lines which is restricted due to economic and environmental reasons. Apart from faster power flow and voltage control in the network, supplementary control is added to these FACTS devices to damp out the interarea oscillations. The conventional damping control synthesis approach considers a single operating condition of the system [2]. The synthesized controllers are tested under different operating conditions with further adjustment of the parameters to satisfy the performance criteria under these conditions before finalizing the design. The controllers obtained from these approaches are simple but, occasionally they are not sufficiently robust to produce adequate damping at other operating conditions, unless they are tuned properly.

Demonstrations of H_∞ based design techniques to power system models has been reported in the literature to guarantee stable and robust operation of the system [3]–[6]. An interesting comparison between various techniques is drawn in [7]. The solution to the H_∞ control design problem based on the Riccati equation approach generally produces a controller that suffers from pole-zero cancellations between the plant and the controller [8]. Furthermore, some of the specifications in the time domain, such as settling time, peak overshoot (closed-loop damping ratio) cannot be captured in a straight forward manner in Riccati-based design [9]. Riccati-based design depends heavily on the proper selection of weights for conditioning the plant. There is no clear procedure for weight selection in power system damping design. The numerical approach to solution through a LMI formulation has distinct advantages since the resulting controller do not in general suffer from the problem of pole-zero cancellation [10]. This is an important consideration since the interarea modes are poorly damped. Application of the LMI approach for damping controller design for PSS has been reported in [11], [12]. PSS is less effective for inter-area mode damping as compared to FACTS devices because the former require phase-lead design with reduced gain margin and the inter-area mode is often poorly controllable from a single unit located at a generator. Moreover, ensuring proper coordination between the various PSSs becomes extremely difficult in deregulated power systems.

Recently, a mixed-sensitivity based LMI approach has been applied to inter-area mode damping employing a superconducting magnetic energy storage (SMES) device [9]. A smaller rated SMES, designed even with high temperature superconductors (HTS)-based materials, is quite costly and, as a result, their large scale application in the network is limited. On the other hand, the controllable phase shifters (CPS), the controllable series capacitors (CSC), the static var compensators (SVC), and other FACTS devices are used by many utilities [13]. This paper addresses the damping design

Manuscript received November 14, 2002. This work was supported in part by ABB, USA, and EPSRC, U.K. under Grant GR/R/31676.

The authors are with the Department of Electrical and Electronic Engineering, Imperial College, London, U.K. (e-mail: b.chaudhuri@ic.ac.uk; b.pal@ic.ac.uk; a.zolotas@ic.ac.uk; i.jaimouka@ic.ac.uk; t.green@ic.ac.uk).

Digital Object Identifier 10.1109/TPWRS.2003.811311

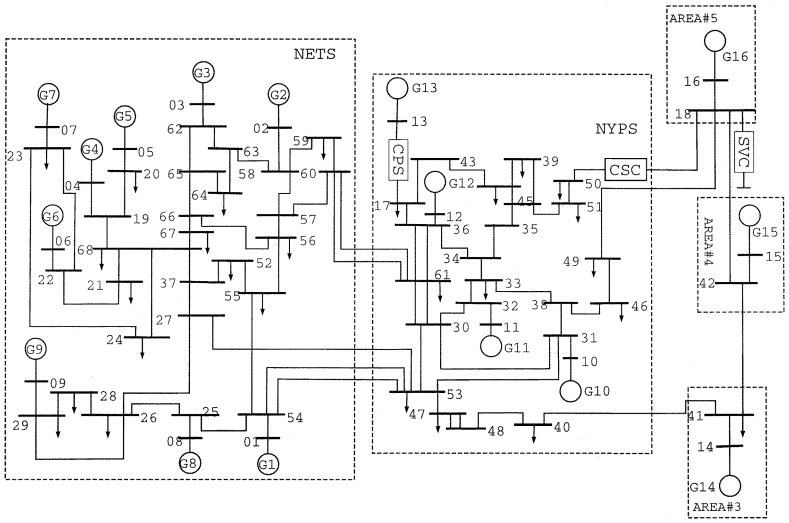

Fig. 1. Sixteen-machine five-area study system.

as an output disturbance rejection problem in an LMI based weighted mixed-sensitivity formulation. Robust damping of multiple inter-area modes employing CSC, SVC, and CPS is the focus of this paper.

II. Study System

A 16-machine, five-area study system, shown in Fig. 1, is considered for damping control design. This is essentially a reduced order model of the New England and New York interconnected system. The tie-lines connecting NETS and NYPS carry 700 MW. Area #5 exports 1550 MW to NYPS and imports 24 MW from Area #4 while 610 MW flows from Area #3 to NYPS and 175 MW from Area #3 to Area #4. The detailed description of the study system including machine, excitation system and network parameters can be found in [14]. The CSC, SVC and CPS are installed in the line between bus #18 and #50, at bus #18 and in the line between bus #13 and #17, respectively. The percentage compensation of the CSC (k_c) is set at 50, the SVC is required to produce 117 MVAR and the phase angle (ϕ) of the CPS is set at 10° to support a desired power-flow through various tie-lines as described earlier.

The prefault steady-state operation of the systems assumes a double circuit tie between bus #53 and #54 and outage of one of these circuits takes the system into postfault steady-state. The results of eigenanalysis displayed in Table II confirms the presence of four interarea modes out of which the first three are poorly damped. A modal residue analysis, suggested in [15], was carried out to identify the most effective local stabilizing signals. The interarea modes were found to be highly observable in the real power flow in the adjacent lines. The normalized modal residues of these signals, displayed in Table I, revealed that the real power flows, $P_{50,51}$, $P_{18,16}$ and $P_{17,13}$ were the best feedback stabilizing signals for the CSC, SVC and CPS respectively. Here $P_{50,51}$, $P_{18,16}$ and $P_{17,13}$ indicate the power-flow in the lines between buses #50–#51, buses #18–#16, and buses #17–#13, respectively.

TABLE I
Normalized Residues for Local Signals

CSC		SVC		CPS	
Line	Residue	Line	Residue	Line	Residue
50-18	0.97	**18-16**	**1.00**	17-36	0.65
50-51	**1.00**	18-50	0.23	17-43	0.11
18-16	0.59	18-49	0.16	**13-17**	**1.00**
-	-	18-42	0.78	-	-

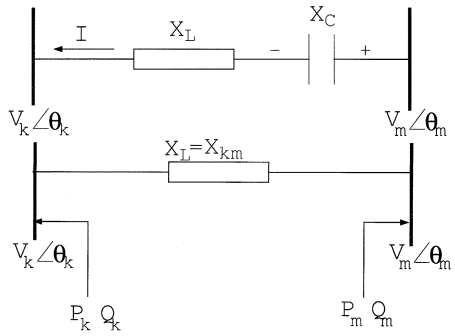

Fig. 2. Power injection model of CSC.

III. FACTS Device Models

The power injection model for different FACTS devices suggested in [16] is used here. In this approach, the effect of FACTS control parameters is modeled as variable power injection at the terminal buses. Fig. 2 shows a typical power injection model of a CSC connected in the line between bus k and m. The effect of the series capacitor (jX_C) is represented by equivalent power injections P_k, Q_k, P_m and Q_m at the terminal buses. The expressions for P_k, Q_k, P_m and Q_m as functions of V_k, V_m, θ_k, θ_m, X_{km} and k_c are described in [16] where, the percentage compensation (k_c) is defined as $k_c = (X_C/X_L) \times 100\%$ where X_L is the reactance of the line. The dynamic characteristics of the CSC is given in Fig. 3 where $\Delta k_{\rm ref}$ is the reference setting which is augmented by $\Delta k_{\rm ss-csc}$ in the presence of supplementary damping control. The reactive power injection of a SVC connected to bus k is given by $Q_k = {V_k}^2 B_{\rm svc}$, where

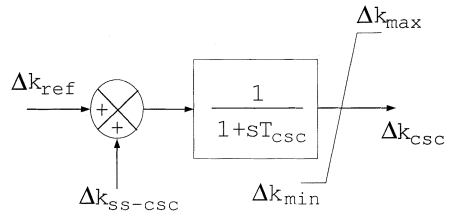

Fig. 3. Small-signal dynamic model of CSC.

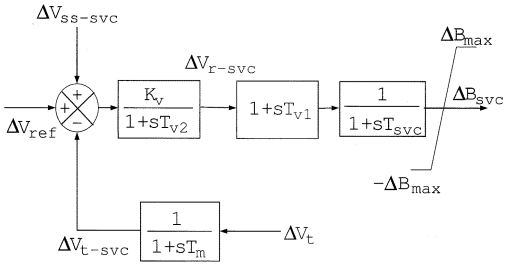

Fig. 4. Small-signal dynamic model of SVC.

$B_{\rm svc} = B_C - B_L$ and B_C and B_L are the susceptance of the fixed capacitor and thyristor controlled reactor, respectively. The small-signal dynamic model of a SVC is given in Fig. 4, where $T_{\rm svc}$ is the response time of the thyristors, T_m is the time constant involved with the measurement hardware and T_{v1} and T_{v2} are the time constants of the voltage regulator block. A CPS is considered to be connected in the line between the bus k and m as shown in Fig. 5. The CPS can be equivalently represented as real and reactive power injections at the terminal buses which are dependent on $V_k, V_m, \theta_k, \theta_m, Z_{km}$ and ϕ, where, ϕ is the phase shifter angle. The small-signal dynamic model of the CPS is given in Fig. 6, where $T_{\rm cps}$ represents the response time of the control circuit and $\Delta\phi_{\rm ref}$ is the reference setting which is augmented by $\Delta\phi_{\rm ss-cps}$ in the presence of supplementary damping control. The device saturations are represented in the small signal models of the CSC, SVC, and CPS by incorporating realistic limits on the output.

A successive relaxation algorithm, discussed in [17], is employed to determine the steady-state settings of these devices to meet the desired line flows. Here, the nodal voltage magnitudes and angles are solved for by the conventional N–R load-flow while a separate sub-problem is solved at the end of each N–R teration to update the state variables for the FACTS in order to meet the specified line flow criteria. The iterative process converges when both the load-flow and the line-flow criteria are satisfied.

The machine, exciter, network power-flow and power injection models for CSC, SVC, and CPS are linearized around the normal operating condition to produce the linear dynamic model for eigen-analysis and control design.

IV. Damping Control Design Formulation: An Output Disturbance Rejection Approach

Oscillations in power systems are triggered by sudden variation on load demand, action of voltage regulator due to fault, etc. These changes appear to FACTS controllers as disturbances.

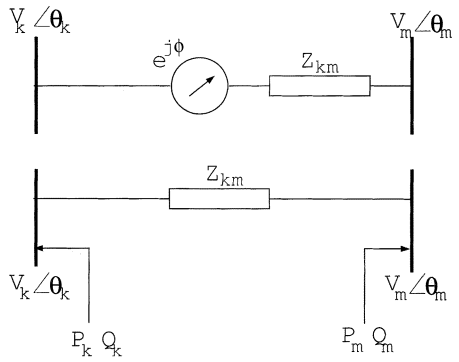

Fig. 5. Power injection model of CPS.

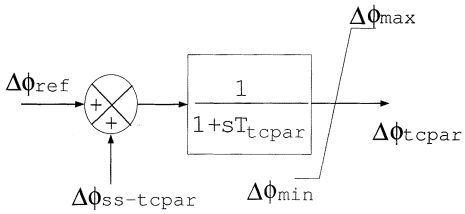

Fig. 6. Small-sensitivity dynamic model of CPS.

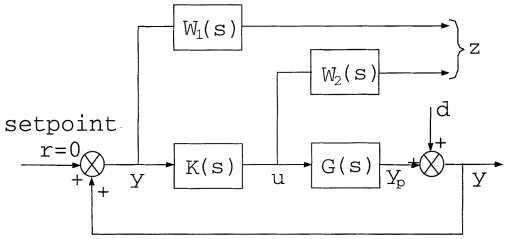

Fig. 7. Mixed-sensitivity output disturbance rejection configuration.

The primary function of the damping controllers is to minimize the impact of these disturbances on the system. The impact of these disturbances in the line active power is highly observable and is represented as a disturbance signal at the plant output. The measured signal, distorted with disturbances, can be used as the controller input. Fig. 7 depicts the output disturbance rejection problem in the standard mixed-sensitivity configuration where $G(s)$ is the open-loop plant, $K(s)$ is the controller to be designed and $W_1(s)$ and $W_2(s)$ are weights for shaping the characteristics of the open-loop plant. The design objective is to minimize a weighted mix of the transfer function $S(s) = (I - G(s)K(s))^{-1}$, which ensures disturbance rejection and $K(s)S(s) = K(s)(I - G(s)K(s))^{-1}$ which handles the robustness issues and minimizes the control effort. This mixed-sensitivity (S/KS) design objective is represented in [18] as

$$\left\| \begin{bmatrix} W_1(s)\,S(s) \\ W_2(s)K(s)S(s) \end{bmatrix} \right\|_\infty < 1. \tag{1}$$

The state-space description of the augmented-plant is given by

$$\begin{bmatrix} \dot{\mathbf{x}}_p \\ \mathbf{z} \\ \mathbf{y} \end{bmatrix} = \begin{bmatrix} A & B_1 & B_2 \\ C_1 & D_{11} & D_{12} \\ C_2 & D_{21} & 0 \end{bmatrix} \begin{bmatrix} \mathbf{x_p} \\ \mathbf{d} \\ \mathbf{u} \end{bmatrix} \tag{2}$$

where $\mathbf{x_p}$: state variable vector of the plant $G(s)$ and weights $(W_1(s), W_2(s))$ combined, $\mathbf{d}$: disturbance input, $\mathbf{u}$: plant input, $\mathbf{y_p}$: plant output, $\mathbf{y}$: measured signals including disturbances, $\mathbf{z}$: regulated output. The state-space representation of the controller is given by

$$\dot{\mathbf{x}}_\mathbf{k} = A_k \mathbf{x_k} + B_k \mathbf{y} \tag{3}$$

$$\mathbf{u} = C_k \mathbf{x_k} + D_k \mathbf{y} \tag{4}$$

where $\mathbf{x_k}$, represents the controller states. $\Delta K_{\mathrm{ss-csc}}$, $\Delta V_{\mathrm{ss-svc}}$ and $\Delta \phi_{\mathrm{ss-cps}}$ are the controller output $(\mathbf{u})$ for CSC, SVC, and CPS, respectively. $\Delta P_{50,51}$, $\Delta P_{18,16}$ and $\Delta P_{17,13}$ are the perturbation of the plant outputs $(\mathbf{y_p})$ $P_{50,51}$, $P_{18,16}$, $P_{17,13}$ around the nominal operating point. The transfer matrix between d and z is given by

$$T_{zd}(s) = \begin{bmatrix} W_1(s)S(s) \\ W_2(s)K(s)S(s) \end{bmatrix} = C_{cl}(sI - A_{cl})^{-1} B_{cl} + D_{cl} \tag{5}$$

where

$$A_{cl} = \begin{bmatrix} A + B_2 D_k C_2 & B_2 C_k \\ B_k C_2 & A_k \end{bmatrix} \tag{6}$$

$$B_{cl} = \begin{bmatrix} B_1 + B_2 D_k D_{21} \\ B_k D_{21} \end{bmatrix} \tag{7}$$

$$C_{cl} = [\, C_1 + D_{12} D_k C_2 \quad D_{12} C_k \,] \tag{8}$$

$$D_{cl} = D_{11} + D_{12} D_k D_{21}. \tag{9}$$

The bounded real lemma, used in [10], with the help of Schur's formula for the determinant of a partitioned matrix [18], allows us to conclude that the closed-loop system in (5) is asymptotically stable if there exists an $X = X^T > 0$ such that

$$\begin{bmatrix} A_{cl}^T X + X A_{cl} & B_{cl} & X C_{cl}^T \\ B_{cl}^T & -I & D_{cl}^T \\ C_{cl} X & D_{cl} & -I \end{bmatrix} < 0. \tag{10}$$

In other words, $\|T_{zd}\|_\infty < 1$, with guaranteed asymptotic stability, is equivalent to the existence of $X = X^T > 0$ that satisfies the LMI condition in (10). The controller design problem then boils down to solving this LMI. However, inequality (10) contains $A_{cl}X$ and $C_{cl}X$, which are products of X and the controller variables, making the problem nonlinear. To convert it to a linear one, a change of controller variables is necessary. The new controller variables are given by (11)–(14) where R, S, M and N are sub-matrices of X[19], [20].

$$\hat{A} = N A_k M^T + N B_k C_2 R + S B_2 C_k M^T + S(A + B_2 D_k C_2) R \tag{11}$$

$$\hat{B} = N B_k + S B_2 D_k \tag{12}$$

$$\hat{C} = C_k M^T + D_k C_2 R \tag{13}$$

$$\hat{D} = D_k. \tag{14}$$

The necessary transformation through substitution of new controller variables requires a solution to the design problem given by

$$\begin{bmatrix} R & I \\ I & S \end{bmatrix} > 0 \tag{15}$$

$$\begin{bmatrix} \Psi_{11} & \Psi_{21}^T \\ \Psi_{21} & \Psi_{22} \end{bmatrix} < 0 \tag{16}$$

where

$$\Psi_{11} = \begin{bmatrix} AR + RA^T + B_2\hat{C} + \hat{C}^T B_2^T & B_1 + B_2 \hat{D} D_{21} \\ \left(B_1 + B_2 \hat{D} D_{21}\right)^T & I \end{bmatrix} \tag{17}$$

$$\Psi_{21} = \begin{bmatrix} \hat{A} + (A + B_2 \hat{D} C_2)^T & S B_1 + \hat{B} D_{21} \\ C_1 R + D_{12} \hat{C} & D_{11} + D_{12} \hat{D} D_{21} \end{bmatrix} \tag{18}$$

$$\Psi_{22} = \begin{bmatrix} A^T S + SA + \hat{B} C_2 + C_2^T \hat{B}^T & \left(C_1 + D_{12} \hat{D} C_2\right)^T \\ C_1 + D_{12} \hat{D} C_2 & -I \end{bmatrix}. \tag{19}$$

The LMIs in (15) and (16) are solved for $\hat{A}$, $\hat{B}$, $\hat{C}$, and $\hat{D}$ as an optimization problem. Once $\hat{A}$, $\hat{B}$, $\hat{C}$, and $\hat{D}$ are obtained, A_k, B_k, C_k, and D_k can be recovered from $\hat{A}$, $\hat{B}$, $\hat{C}$, and $\hat{D}$ by solving the (11)–(14).

V. Damping Controller Design

The LMI formulation in Section IV produces centralized controllers in multivariable form. The centralized controllers produce acceptable damping ratios using less control effort as compared to the decentralized ones. The disturbance rejection performance of the controllers, when tested through nonlinear simulation, has been found inadequate because of possible interactions among off-diagonal entries in the centralized controller [7], [9]. Moreover centralized control requires dedicated communication links for transmitting signals which invariably introduces time delay. Here, the design of the damping controllers is done in a sequential manner using a decentralized approach i.e., once the damping controller for one device is designed the loop is closed before designing the next one. At each stage of this sequential design, the plant model is updated with the controller model. In order to expedite the solution process in the LMI routine, the plant order has to be reduced before the controller design can be carried out. The study system has 138 states in the open-loop. In sequential design, this number will increase as each loop is closed depending on the number of states associated with the controllers of these devices. At each stage of the sequential design, the original plant is reduced to a 10–12th order plant. The *Robust Control Toolbox* available with Matlab has been used to perform the necessary computations. Balanced truncation [18] is used for reduction of the model. Such large order reduction is justified as long as the input–output characteristics in the desired frequency range are reasonably close to that of the full order system. For both the prefault and postfault operating conditions, an order of 10 was found to be satisfactory. The singular value response of the input–output characteristics of the CSC for the full order and the reduced order plant, shown in Fig. 8, demonstrates that the reduced 10th order plant is very close to the full 138th order plant. Model reductions of the plants for CPS and SVC to the same order showed a similar degree of agreement between the singular value characteristics of the full and reduced order plant. The standard practice in a Riccati based approach is to choose the weight $W_1(s)$ as a high gain low pass filter for output disturbance rejection. The weight $W_2(s)$ should be a

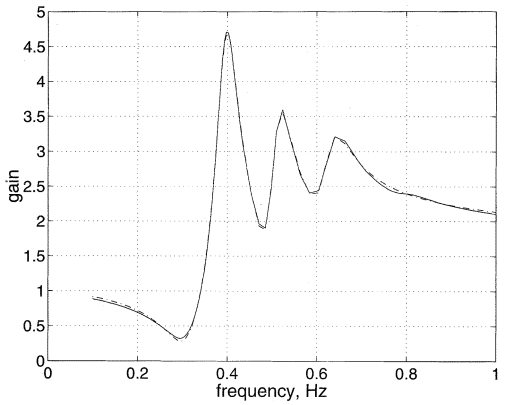

Fig. 8. Frequency response plots of the input–output characteristics for CSC. (-) reduced; (--) full order.

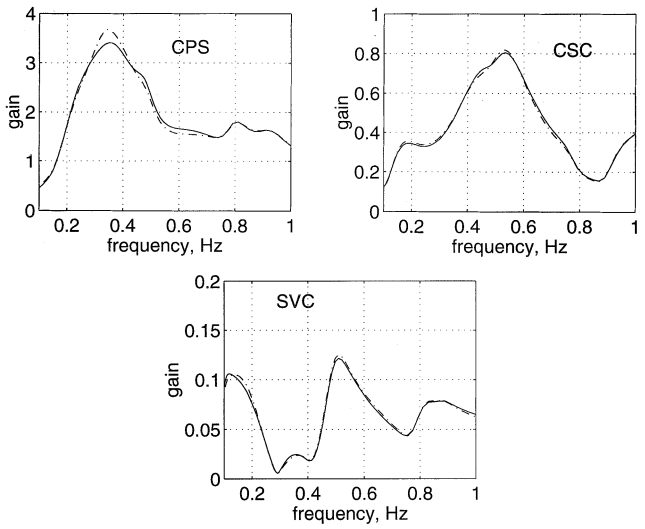

Fig. 9. Closed loop frequency response (full plant) with; (-) reduced order controller; (--) full order controller.

high-pass filter in order to reduce the control effort and to ensure robustness against additive uncertainties in the plant model in the high frequency range. As a starting point, we choose the same shape of weights $W_1(s)$ and $W_2(s)$ used in [9] for SMES design. A scale factor of 0.8475 is found to suit the design requirement for CSC, SVC and CPS. The weights W_1 and W_2 are given by

$$W_1(s) = 0.8475\frac{99s + 11\,400}{s^2 + 156s + 12504} \tag{20}$$

$$W_2(s) = 0.8475\frac{0.1055s^2 + 0.037s + 0.0094}{s(s + 0.0020)^2}. \tag{21}$$

The multiobjective (disturbance rejection and control effort optimization) feature of LMI is accessed through suitably defining the objective in the argument of the function *hinfmix* of the *LMI Toolbox* [21] in Matlab. The sequential design of the controllers for CSC, SVC and CPS has been carried out in the respective sequence. The choice of this sequence improves the damping of modes #1, #2 and #3 in that order, respectively. The other sequences produced slightly different controllers but essentially the same performance was achieved. The same set of weights given in (20) and (21) has been found to work well for the design of the controllers. One of the drawbacks of the LMI based design is that the order of the controllers obtained from the LMI solution is equal to the reduced plant order plus the order of the weights, which is quite high from a practical implementation point of view. Therefore the controllers are reduced to 5th order by balanced truncation without significantly affecting the frequency response. These reduced order controllers were tested on the original system (full order) for both prefault and postfault operating conditions. The selected weights $W_1(s)$ and $W_2(s)$ enabled us to produce proper control structure that moved the closed-loop interarea modes further toward the left-half plane. The gain of the controllers (but not the controller structure) were scaled slightly to produce a damping ratio which ensured settling of oscillations in 10–12 s, as viewed in the linear simulation using the function *lsim* in Matlab. In our exercise the change of gain required was small. The transfer functions of the designed controllers are given below

$$\begin{aligned}
K_{\rm CSC}(s) =& K_{\rm CSC}\frac{N_{\rm CSC}(s)}{D_{\rm CSC}(s)}\\
K_{\rm CSC} =& 1.05\\
N_{\rm CSC}(s) =& -4.88\times 10^5 s^4 - 2.33\times 10^8 s^3\\
&- 2.76\times 10^9 s^2 - 1.55\times 10^{10} s + 1.56\times 10^9\\
D_{\rm CSC}(s) =& s^5 + 2.14\times 10^5 s^4 + 1.77\times 10^8 s^3\\
&+ 1.32\times 10^{10} s^2 + 6.51\times 10^9 s + 2.38\times 10^{10}\\
K_{\rm SVC}(s) =& K_{\rm SVC}\frac{N_{\rm SVC}(s)}{D_{\rm SVC}(s)}\\
K_{\rm SVC} =& 2.70\\
N_{\rm SVC}(s) =& 8.36\times 10^3 s^4 + 7.51\times 10^6 s^3\\
&- 3.31\times 10^7 s^2 + 1.27\times 10^9 s - 3.43\times 10^8\\
D_{\rm SVC}(s) =& s^5 + 7.79\times 10^3 s^4 + 9.47\times 10^6 s^3\\
&+ 5.35\times 10^8 s^2 + 1.71\times 10^9 s + 2.09\times 10^9\\
K_{\rm CPS}(s) =& K_{\rm CPS}\frac{N_{\rm CPS}(s)}{D_{\rm CPS}(s)}\\
K_{\rm CPS} =& 1.00\\
N_{\rm CPS}(s) =& 1.02\times 10^6 s^4 + 1.83\times 10^9 s^3\\
&+ 1.01\times 10^{11} s^2 + 3.05\times 10^{11} s + 5.36\times 10^{10}\\
D_{\rm CPS}(s) =& s^5 + 8.94\times 10^5 s^4 + 8.87\times 10^9 s^3\\
&+ 3.69\times 10^{12} s^2 + 2.56\times 10^{12} s + 2.26\times 10^{12}.
\end{aligned}$$

It can be noted from Fig. 9 that the controller reduction procedure has very little effect on the closed-loop frequency response.

VI. Evaluation of Controller Performance

The eigen-analysis of the study system was carried out for various scenarios. The results are shown in Tables II–VII for several operating conditions. It is clear from these results that the damping ratios of the inter-area modes in the presence of the three controllers are improved considerably. Although the damping of the fourth mode looks low, it is adequate as the time domain simulation shows that oscillations influenced by this mode settle in 10–12 s. Table II contains the results with only the controller for CSC considered. It can be seen that the damping of mode #1, shown in boldface, is improved primarily with very

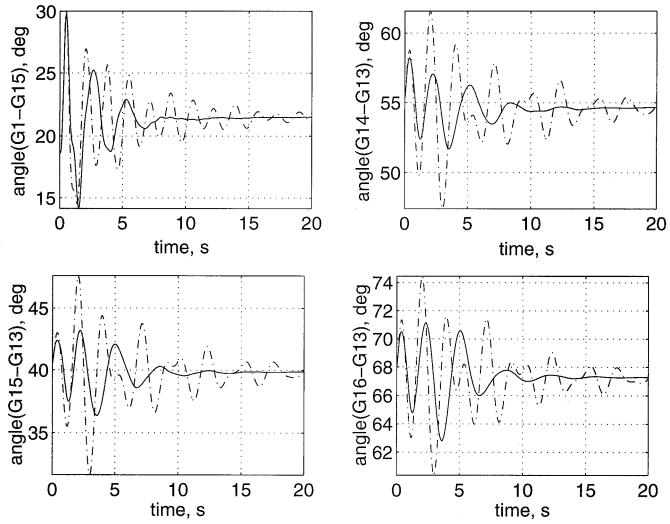

Fig. 10. Dynamic response of the system following fault at bus #53 (-) with controller; (-·) without controller.

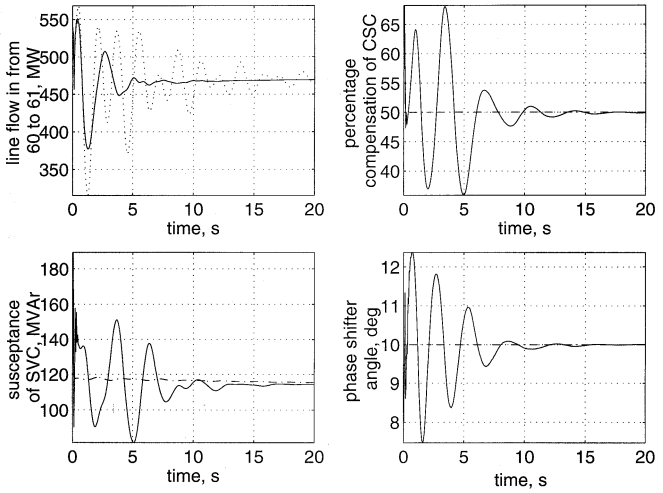

Fig. 11. Dynamic response of the system following fault at bus #53 (-) with controller; (··) without controller.

little effect on modes #2, #3, and #4. Similarly, Table III shows that the controller for SVC primarily improves the damping of mode #2, shown in boldface, besides improving mode #1 slightly. The controller for CPS primarily improves the damping of mode #3, shown in boldface, besides adding to the damping ratios of modes #1 and #2 as evidenced in Table IV. The action of the three controllers has been found to improve the damping of all the three critical inter-area modes to adequate level. The damping action of the controllers was examined at different power flow levels. Table V displays the damping ratios and frequencies of the interarea modes when power flow from NETS to NYPS varies in the range 100–900 MW. The performance of the controllers was evaluated with various load models. Constant impedance (CI), constant power (CP), constant current (CC), and dynamic load characteristics are considered. The dynamic load (induction motor type) is considered to be at bus #41, the rest being of CI type. It is clear from the results of Table VI that the designed controllers provide robust damping for different load characteristics. Table VII demonstrates the robustness of the damping action in case of outage of different tie-lines connecting NETS and NYPS. The damping action is shown to be quite robust with respect to the outage of each of the tie-lines between buses #27–#53, buses #60–#61, and buses #53–#54 which connects NETS and NYPS.

A nonlinear simulation has been carried out for 30 s to further demonstrate performance robustness of the controllers in the presence of system nonlinearities, including saturation. One of the most probable contingencies of the system with respect to interarea power transfer is a three-phase bolted fault near bus #53 on one of the tie-lines connecting buses #53–#54. The fault at this location is certainly not the most severe one as far as the transient stability implications are concerned but it is effective for exciting inter-area oscillations and examining the performance of the damping controllers. The fault was simulated for 80 ms ($\approx$ 5 cycles) followed by opening of the faulted line. The dynamic response of the system following this contingency is shown in Figs. 10 and 11. The displays in Fig. 10 show the relative angular separation of machines #1, #14, #15, and #16 from that of machine #13. It can be seen that the interarea oscillations are damped out in 10–15 s. A 10–15-s settling is adopted by many utilities in their system design and operation guidelines [1]. Fig. 11 shows the power flow in the tie-line connecting buses #60–#61 and also the output responses of the CSC, SVC, and CPS following a disturbance. It can be seen that the oscillation in the power flow is settled within 10–15 s and the outputs of the CSC, SVC, and CPS are well within their prescribed limits. The dynamic response also shows that adverse interactions between different control loops are absent. Thus, the large

TABLE II
DAMPING RATIOS AND FREQUENCIES OF INTERAREA MODES WITH THE CONTROLLER FOR CSC (CONTROL LOOPS FOR SVC AND CPS OPEN)

Mode No.	Pre-fault				Post-fault			
	Open-loop		Closed-loop		Open-loop		Closed-loop	
	ζ	f(Hz)	ζ	f(Hz)	ζ	f(Hz)	ζ	f(Hz)
1	**0.0626**	0.3945	**0.1544**	0.3434	**0.0513**	0.3759	**0.1310**	0.3288
2	0.0434	0.5105	0.0545	0.4991	0.0422	0.5094	0.0543	0.5002
3	0.0560	0.6269	0.0656	0.6191	0.0476	0.5978	0.0618	0.5841
4	0.0499	0.7923	0.0502	0.7918	0.0499	0.7920	0.0502	0.7914

TABLE III
DAMPING RATIOS AND FREQUENCIES OF INTERAREA MODES WITH THE CONTROLLERS FOR CSC AND SVC (CONTROL LOOP FOR CPS OPEN)

Mode No.	Pre-fault				Post-fault			
	Open-loop		Closed-loop		Open-loop		Closed-loop	
	ζ	f(Hz)	ζ	f(Hz)	ζ	f(Hz)	ζ	f(Hz)
1	0.1544	0.3434	0.1795	0.3158	0.1310	0.3288	0.1464	0.3060
2	**0.0545**	0.4991	**0.1031**	0.4549	**0.0543**	0.5002	**0.1091**	0.4536
3	0.0656	0.6191	0.0643	0.6184	0.0618	0.5841	0.0584	0.5835
4	0.0502	0.7918	0.0603	0.7864	0.0502	0.7914	0.0603	0.7860

TABLE IV
DAMPING RATIOS AND FREQUENCIES OF INTERAREA MODES WITH THE CONTROLLERS FOR CSC, SVC, AND CPS (ALL CONTROL LOOPS CONSIDERED)

Mode No.	Pre-fault				Post-fault			
	Open-loop		Closed-loop		Open-loop		Closed-loop	
	ζ	f(Hz)	ζ	f(Hz)	ζ	f(Hz)	ζ	f(Hz)
1	0.1795	0.3158	0.3140	0.2682	0.1464	0.3060	0.2784	0.2709
2	0.1031	0.4549	0.2266	0.4444	0.1091	0.4536	0.2060	0.4091
3	**0.0643**	0.6184	**0.1105**	0.4585	**0.0584**	0.5835	**0.1076**	0.4539
4	0.0603	0.7864	0.0600	0.7858	0.0603	0.7860	0.0601	0.7848

TABLE V
DAMPING RATIOS AND FREQUENCIES OF INTERAREA MODES AT DIFFERENT LEVELS OF POWER FLOW BETWEEN NETS AND NYPS

Power flow (MW)	Mode 1		Mode 2		Mode 3		Mode4	
	ζ	f(Hz)	ζ	f(Hz)	ζ	f(Hz)	ζ	f(Hz)
100	**0.3362**	0.2610	**0.2066**	0.4545	**0.1184**	0.4904	0.0602	0.7858
500	**0.3210**	0.2658	**0.2201**	0.4576	**0.1144**	0.4618	0.0601	0.7858
700	**0.3140**	0.2682	**0.2266**	0.4444	**0.1105**	0.4585	0.0600	0.7858
900	**0.3072**	0.2705	**0.2246**	0.4247	**0.1065**	0.4584	0.0600	0.7857

TABLE VI
DAMPING RATIOS AND FREQUENCIES OF INTERAREA MODES FOR DIFFERENT LOAD CHARACTERISTICS

Type of load	Mode 1		Mode 2		Mode 3		Mode4	
	ζ	f(Hz)	ζ	f(Hz)	ζ	f(Hz)	ζ	f(Hz)
CI	**0.3140**	0.2682	**0.2266**	0.4444	**0.1105**	0.4585	0.0600	0.7858
CC	**0.2950**	0.2664	**0.1864**	0.4774	**0.1114**	0.4859	0.0598	0.7885
CP	**0.2212**	0.2671	**0.1858**	0.4214	**0.1028**	0.4721	0.0582	0.7916
Dynamic	**0.3120**	0.2682	**0.2274**	0.4436	**0.1288**	0.4582	0.0639	0.7856

TABLE VII
DAMPING RATIOS AND FREQUENCIES OF INTERAREA MODES FOR DIFFERENT TIE-LINE STRENGTHS

Outage of tie-line	Mode 1		Mode 2		Mode 3		Mode4	
	ζ	f(Hz)	ζ	f(Hz)	ζ	f(Hz)	ζ	f(Hz)
60-61	**0.2824**	0.2727	**0.1829**	0.4065	**0.1050**	0.4555	0.0600	0.7851
53-54	**0.2784**	0.2709	**0.2060**	0.4091	**0.1076**	0.4539	0.0601	0.7848
27-53	**0.3021**	0.2687	**0.2263**	0.4330	**0.1086**	0.4570	0.0601	0.7854

disturbance performance of the controllers is found to be highly acceptable.

VII. CONCLUSIONS

We have formulated the damping control design in power systems as a multi-objective optimization problem in the LMI framework. The mixed-sensitivity objective addresses both output disturbance rejection and minimizes control effort. The solution is numerically sought through the LMI solver. We have applied the mixed-sensitivity based damping design methodology introduced in [9] to CSC, SVC and CPS. It is found that mixed-sensitivity based H_∞ damping control design through the LMI approach is successful for several FACTS devices. The technique has been found to work satisfactorily for three study systems employing these devices. One interesting finding of our research is the apparent standardization of the weights for shaping the open loop plant involving different FACTS devices with real power flow in the line as stabilizing signals. Through proper selection of stabilizing signals, it is possible to find a plant transfer function which shows a peak around the critical frequency range (i.e., 0.2–1.0 Hz). This is true for each type of FACTS device and even for larger systems making the design problems somewhat similar and hence a similar shape of weights has been found to work in the mixed-sensitivity based design formulation. The same set of weights does not necessarily provide the most cost-effective controller for each and every FACTS device, but it certainly produces the desirable damping ratios for the interarea modes. The performance robustness of the designed controllers has been verified in the frequency domain through eigen-analysis and also in the time domain through nonlinear simulations. The nonlinear response has also verified that adverse interactions between different control loops are absent. We believe that the main contribution of this paper is in adopting an output disturbance rejection approach for formulating the control design problem and clearly demonstrating the effectiveness of the control algorithm in tackling a realistic study system involving multiple FACTS devices, commonly used in practice, operating under a wide range of conditions.

One disadvantage of the decentralized design using local signals is that supplementary damping control action through three FACTS devices is necessary to improve the damping of the three dominant inter-area modes. But in practical systems, the number of dominant inter-area modes is often larger than the number of control devices available. In those case centralized design with global signals, containing diverse modal content, may address the problem and is, therefore, the focus of our future research. For practical study systems, the number of states is often more than 1000. For those systems it might be difficult to employ the standard model reduction techniques available with *Robust Control Toolbox* in Matlab because they require the explicit solution of Lyapunov equations, which might be difficult for larger systems. Krylov-subspace based model reduction algorithms [22] have been applied for simplification of very large systems in several process control applications. We intend to apply this technique for simplification of large power system models to validate our design techniques for practical systems.

REFERENCES

[1] J. Paserba, *Analysis and Control of Power System Oscillation*: CIGRE Special Publication 38.01.07, 1996, vol. Technical Brochure 111.
[2] P. Kundur, *Power System Stability and Control*. New York: McGraw-Hill, 1994.

[3] M. Klein, L. Le, G. Rogers, S. Farrokpay, and N. Balu, "H_∞ damping controller design in large power system," *IEEE Trans. Power Syst.*, vol. 10, pp. 158–166, Feb. 1995.
[4] Q. Zhao and J. Jiang, "Robust SVC controller design for improving power system damping," *IEEE Trans. Power Syst.*, vol. 10, pp. 1927–1932, Nov. 1995.
[5] I. Kamwa, G. Trudel, and L. Gérin-Lajoie, "Robust design and coordination of multiple damping controllers using nonlinear constrained optimization," *IEEE Trans. Power Syst.*, vol. 15, pp. 1084–1092, Aug. 2000.
[6] G. Taranto and J. Chow, "A robust frequency domain optimization technique for tuning series compensation damping controllers," *IEEE Trans. Power Syst.*, vol. 10, pp. 1219–1225, Aug. 1995.
[7] G. Boukarim, S. Wang, J. Chow, G. Taranto, and N. Martins, "A comparison of classical, robust and decentralized control designs for multiple power system stabilizer," *IEEE Trans. Power Syst.*, vol. 15, pp. 1287–1292, Nov. 2000.
[8] J. Sefton and K. Glover, "Pole/zero cancellations in the general H_∞ problem with reference to a two block design," *Systems and Control Letters*, vol. 14, pp. 295–306, 1990.
[9] B. Pal, A. Coonick, I. Jaimoukha, and H. Zobaidi, "A linear matrix inequality approach to robust damping control design in power systems with superconducting magnetic energy storage device," *IEEE Trans. Power Syst.*, vol. 15, pp. 356–362, Feb. 2000.
[10] P. Gahinet and P. Apkarian, "A linear matrix inequality approach to H_∞ control," *Int. J. Robust and Non-linear Control*, vol. 4, pp. 421–448, 1994.
[11] P. Rao and I. Sen, "Robust pole placement stabilizer design using linear matrix inequalities," *IEEE Trans. Power Syst.*, vol. 15, pp. 313–319, Feb. 2000.
[12] G. Taranto, S. Wang, J. Chow, and N. Martins, "Decentralized design of power system damping controllers using a linear matrix inequality algorithm," in *Proc. VI SE-POPE*, 1998.
[13] Y. Song and A. Johns, *Flexible AC Transmission Systems*, ser. Inst. Elect. Eng. Power and Energy, 1999.
[14] G. Rogers, *Power System Oscillations*. Norwell, MA: Kluwer , 2000.
[15] N. Martins and L. Lima, "Determination of suitable locations for power system stabilizers and static var compensators for damping electromechanical oscillations in large power systems," *IEEE Trans. Power Syst.*, vol. 5, pp. 1455–1469, Nov. 1990.
[16] M. Noroozian, L. Angquist, M. Gandhari, and G. Andersson, "Improving power system dynamics by series-connected FACTS devices," *IEEE Trans. Power Delivery*, vol. 12, pp. 1635–1641, Oct. 1997.
[17] M. Noroozian and G. Andersson, "Power flow control by use of controllable series components," *IEEE Trans. Power Delivery*, vol. 8, pp. 1420–1429, July 1993.
[18] S. Skogestad and I. Postlethwaite, *Multivariable Feedback Control*. New York: Wiley, 2001.
[19] M. Chilali and P. Gahinet, "Multi-objective output feedback control via LMI optimization," *IEEE Trans. Automat. Contr.*, vol. 42, pp. 896–911, July 1997.
[20] C. Scherer, P. Gahinet, and M. Chilali, "H_∞ design with pole placement constraints: An LMI approach," *IEEE Trans. Automat. Contr.*, vol. 41, no. 3, pp. 358–367, Mar. 1996.
[21] P. Gahinet, A. Nemirovski, A. Laub, and M. Chilali, *LMI Control Toolbox for Use With Matlab*: The Math Works Inc., 1995.
[22] I. Jaimoukha and E. Kasenally, "Implicitly restarted Krylov subspace methods for stable partial realizations," *SIAM J. Matrix Anal. Applicat.*, vol. 18, no. 3, pp. 633–652, 1997.

Balarko Chaudhuri received the B.E.E. (Hons.) degree from Jadavpur University, India, in 2000, and the M.Tech degree from the Indian Institute of Technology, Kanpur, India, in 2002. He is currently pursuing the Ph.D. degree in the control and power group at Imperial College, London, U.K.

Bikash C. Pal received the B.E.E. (Hons.) degree from Jadavpur University, India, in 1990, and the M.E. degree from the Indian Institute of Science in 1992. He received the Ph.D. degree from Imperial College, London, U.K., in 1999.

Currently, he is a Lecturer in the Department of Electrical and Electronic Engineering, Imperial College, London, U.K. His research interest includes the area of power system dynamics and control of FACTS devices.

Argyrios C. Zolotas graduated from Leeds University, U.K., in 1998 and received the Ph.D. degree in 2002 from Loughborough University, U.K. He is currently a Post-Doctoral fellow in the Department of Electrical and Electronic Engineering, Imperial College, London, U.K.

His research interests are in robust control, LMIs, active suspensions, large-scale models, and model reduction.

Imad M. Jaimoukha graduated from the University of Southampton, U.K., in 1983, and received the Ph.D. degree in 1990 from Imperial College, London, U.K.

Currently, he is a Senior Lecturer in the Department of Electrical and Electronic Engineering, Imperial College, London, U.K. His research interests include robust multivariable control and model reduction.

Tim C. Green graduated from Imperial College, London, U.K., in 1986 and received the Ph.D. degree from Heriot-Watt University, Edinburgh, U.K., in 1990. Currently, he is a Senior Lecturer at Imperial College, London, U.K., and deputy head of the Control and Power research group.

His research interests lie in the application of power electronics to power systems.